Advanced Composites and Hybrid Materials (2018) 1:135–148
https://doi.org/10.1007/s42114-017-0019-9

ORIGINAL RESEARCH

Reduced graphene oxide-coated cotton as an efficient absorbent in oil-water separation

Love Dashairya[1] · Madhabendra Rout[1] · Partha Saha[1]

Received: 25 October 2017 / Accepted: 27 November 2017 / Published online: 7 December 2017

Abstract

The present work describes the fabrication of superhydrophobic and superoleophilic reduced graphene oxide-coated cotton (rGO@cotton) by a facile one-step hydrothermal used method for oil-water separation. Results from X-ray diffraction (XRD), Fourier transform infrared spectroscopy (FTIR), and field emission scanning electron microscopy (FESEM) analysis show the formation of a composite structure with the presence of an ultrathin coating of rGO on the cotton fibers. The contact angle (CA) between a static water droplet and the rGO@cotton surface in air was measured ~ 162.9°, which suggests the formation of a superhydrophobic surface on the synthesized product. Moreover, the rGO@cotton showed excellent absorption capacity for oils where 1 g of rGO@cotton was able to remove ~ 30–40 g of various oils in the first cycle from oil-water mixtures. The flexible rGO@cotton was reusable and demonstrated oil retention up to ~ 35–50% at the tenth cycle using simple sorption-mechanical squeezing test. Overall, the present work identifies that the rGO@cotton is an efficient absorbent for effective separation of oil from oil-water mixtures.

Keywords Reduced graphene oxide · Cotton · Superhydrophobicity · Contact angle · Absorption · Recyclability

1 Introduction

Over the last few decades, water pollution through the oil spill, and industrial waste such as crude oil, petroleum by-products, and hazardous organic solvents from chemical industries have posed a severe threat to the humanity and marine lives with growing ecological and environmental concerns throughout the world [1, 2]. Moreover, most of the oil spill accidents occurred in the sea during oil extraction, transportation, and storage. To date, oil spill remains a real threat to natural habitats, and there are few solutions to resolve this problem. Traditional methods of centrifugation, oil skimmer, flotation, and gravitational separation suffer due to poor efficiency and long cycle times for efficient separation of oil from water [3, 4]. Also, conventional remedies like mechanical extraction, chemical degradation, and in situ burning for massive oil spills are inefficient and require high operational cost [5]. Traditional hydrophobic/oleophilic materials studied for the removal and collection of oil have limits such as low absorption capacity, the high cost of fabrication, and poor reusability. Notably, some materials absorb water and oil simultaneously, which indicate a weak hydrophobicity and low oil-water separation efficiency [6].

In recent times, superhydrophobic (contact angle > 150°)-based and superoleophilic (contact angle < 10°)-based materials explored for oil separation or hazardous organic solvent clean-up from the oil-water mixture owing to their excellent

Love Dashairya and Madhabendra Rout contributed equally to this work.

Highlights
- rGO@cotton-based superhydrophobic material is developed by hydrothermal method.
- A composite structure with an ultrathin coating of rGO on cotton fibers is formed.
- The contact angle (CA) measurement between a static water droplet and rGO@cotton surface in air shows CA ~ 162.9°, which suggests the superhydrophobicity of the material.
- The rGO@cotton can remove ~50–60 times various oils of its weight by simple sorption-mechanical squeezing test.

Electronic supplementary material The online version of this article (https://doi.org/10.1007/s42114-017-0019-9) contains supplementary material, which is available to authorized users.

✉ Partha Saha
sahapartha29@gmail.com; sahap@nitrkl.ac.in

[1] Department of Ceramic Engineering, National Institute of Technology, Rourkela, Odisha 769008, India

selectivity, high absorption capacities, stability, and recyclability [7, 8]. In this regards, metal oxide, inorganic clay, magnetic materials, polymer microfiber bundles, polymer-based superhydrophobic materials, and sponge-like aerogels have been explored for oil-water separation because of its high surface area, coupled with excellent mechanochemical stability, and hydrophobicity [4, 9–13]. In addition, metal meshes have also been reported explored for oil-water separation but have limitations of low separation efficiency and poor cyclability [14, 15]. However, the high cost of the chemicals required for the synthesis of above materials and associated environmental and ecological concerns restrict their widespread use [16, 17].

Over the last few years, carbonaceous materials such as carbon nanotubes [18], carbon black [19], expanded graphite [10, 20], graphene aerogels [21, 22], reduced graphene oxide (rGO) [23], and carbon nanofibers [24] have emerged as materials of choice for oil spill clean-up owing to their excellent non-wettability towards water. Among all, graphene-based sorbents have attracted significant attention for oil-water separation due to their ease of fabrication, superhydrophobicity, and high surface area, along with excellent chemical, thermal, and mechanical stability [25, 26]. Graphene, generally obtained by chemical oxidation of graphite to graphene oxide (GO) followed by chemical/thermal reduction to graphene or reduced graphene oxide (rGO), demonstrates excellent sorption behavior [27, 28]. Interestingly, GO displays hydrophilic nature due to the presence of oxygen-rich functional groups (carboxylic, hydroxyl, and epoxy groups) protruding out from the two-dimensional ring structure. On the contrary, rGO shows hydrophobic behavior due to the absence of any functional groups [29, 30]. Recently, rGO/cotton fabric [23], rGO/membrane [31], and rGO/polyurethane-based sponges [32] have shown promise as sorbents for oil-water separation. Gupta and Tai [9] recently reviewed various carbonaceous-based compounds as oil absorption materials which highlight that rGO or graphene has superior oil absorption capacities. Sun et al. [23] demonstrated rGO-coated cotton functionalized by polydimethoxysilane could remove oils ~11–25 times of its weight. Ge et al. [33] reported ~30–50 times absorption capacities for various oils using rGO-coated cotton. Upadhyay et al. [34] showed rGO-coated sparse cloth is capable of oil-water separation with absorption capacity ~10 times of its weight. Liu et al. [31] reported polydopamine-coated rGO membranes for oil-water emulsions separation. Most recently, graphene-wrapped sponge displayed ~ 94.6% oil-water separation efficiency [35], and polymer/rGO sponges [36], spongy graphene aerogel [37], and rGO foam [38] exhibited excellent superhydrophobicity and selective oil absorption. Wang et al. [39] reported a drop-coating method for the fabrication of superhydrophobic/superoleophilic cotton textile using stearic acid modified ZnO particles and polystyrene. Zhou et al. [40] modified cotton fabrics using polyaniline and fluorinated alkyl silane by a vapor phase deposition process render it superhydrophobic/superoleophilic for oil-water separation. From the above literature, it appears that cotton-based materials with surface modified by rGO or graphene have tremendous promise as sorbents for oil-water separation. Cotton is a natural plant fiber which is porous, soft, and flexible, and possesses excellent mechanical stability and ideal for a supporting host in a three-dimensional porous structure. Therefore, there is a merit to fabricate cotton-based hydrophobic/oleophilic materials for efficient oil-water separation.

Herein, we report a facile single-step hydrothermal method for the preparation of superhydrophobic/superoleophilic cotton modified by rGO (rGO@cotton) as an active sorbent for oil-water separation with water contact angle (CA) ~ 162.9°. Firstly, the pristine cotton immersed in GO solution that allows complete wetting of each fiber. The dried and as-prepared GO@cotton was hydrothermally treated using hydrazine hydrate as a reducing agent to prepare the rGO@cotton material. The composite rGO@cotton repelled water entirely while at the same time allowed complete permeation of oils and organic solvents for effective separation of the oil-water mixture. Importantly, the as-prepared rGO@cotton maintained separation efficiency ~ 30–60 g/g of its weight and excellent reusability for ten cycles. Furthermore, the rGO@cotton can withstand a temperature up to 150 °C with superhydrophobicity, and superoleophobicity properties remain unchanged which demonstrates the versatility of the synthesized product for efficient oil-water separation.

2 Experimental

All the chemicals were analytical grade reagents without further purification. De-ionized water was used throughout the synthesis and experiments. Acetone, propanol, dimethylformamide (DMF), and *n*-methyl-pyrrolidone (NMP) were obtained from Loba Chemie India. H_2SO_4, $NaNO_3$, $KMnO_4$, and H_2O_2 were purchased from Merck, India. Organic dye (oil red IV, practical grade) was purchased from HiMedia Laboratories Pvt. Ltd. The pristine cotton, engine oil, and pump oil were procured from a local store. The natural graphite flakes and hydrazine hydrate (99%) were provided by Thermo Fisher Scientific India Pvt. Ltd.

2.1 Synthesis of graphene oxide

Graphene oxide (GO) was synthesized from natural graphite by a modified Hummers method [27, 28, 41]. Briefly, 3 g graphite powder and 1.5 g $NaNO_3$ was added into 70 ml of H_2SO_4. Then, the mixture was cooled in an ice bath. Nine grams of $KMnO_4$, acting as an oxidizing agent, was gradually

added while stirring. The reaction temperature was maintained below 20 °C by carefully controlling the rate of addition and continuously stirred for 12 h. Subsequently, the reaction mixture was diluted with distilled water in an ice bath, and the temperature rapidly increased to 90 °C. Further, the suspension stirred at 90 °C for 1 day and 3 ml H_2O_2 was added to terminate the reaction. The solid GO thus obtained was filtered followed by centrifugation and washed several times with 5% HCl, distilled water, and ethanol, respectively. The resulting brown color precipitate was dried in vacuum oven at 60 °C for 12 h.

2.2 Synthesis of reduced graphene oxide-coated cotton

First, a cotton ball was treated with acetone and distilled water, followed by drying at 60 °C for 4 h. Then, the pretreated cotton was dipped into a 150 ml exfoliated GO aqueous solution to wrap each cotton fiber entirely by GO. To determine the maximum absorption capacity of the reduced graphene oxide-coated cotton (rGO@cotton), a sequence of synthesis was carried out by varying the concentration of GO (0.5, 1, 1.5, 2, and 2.5 mg ml^{-1}) in cotton. Then, the GO@cotton solution was filled into a 200 ml Teflon-lined stainless steel autoclave and hydrothermally treated using hydrazine hydrate as reducing agent at 90 °C for 12 h. Finally, the rGO@cotton thus obtained was kept in an oven at 110 °C for complete removal of moisture. For the preparation of rGO, the same synthesis method was repeated without the cotton.

2.3 Absorption capacity and recyclability test

The absorption capacity can be expressed by the ratio of the weight gains to initial weight of rGO@cotton. The absorption capacity was defined as follows:

$$\textit{Absorption capacity}\ (\mathrm{AC}) = (W_f - W_i)/W_i$$

where W_i and W_f are the weight of the rGO@cotton before and after absorption, respectively. To evaluate the absorption capacity, equal weight (~ 200 mg) of rGO@cotton was taken for all the experiments. First, the rGO@cotton was immersed in the mixture of oil/organic solvent with water with a volume:volume ratio of 1:4, and the absorption capacity was determined by immediate value taken at 0 min for each cycle. The initial weight of rGO@cotton was noted as W_i, and after immersion in different media, it was noted as W_f. The oil-loaded rGO@cotton was mechanically squeezed to release the oil/organic solvent, and the residual weight was noted as W_r, to calculate the collection efficiency. The absorption/collection capacity was repeated for ten cycles with three measurements for each period to evaluate the reusability of the rGO@cotton [42].

$$\textit{Collection capacity}\ (\mathrm{CC}) = (W_r - W_i)/W_i$$

Here, W_r = residual weight of rGO@cotton after desorption.

2.4 Material characterization

GO, rGO, pristine cotton, and rGO@cotton were characterized by X-ray diffraction (XRD), field emission scanning electron microscopy (FESEM), thermogravimetric (TG) analysis, and Fourier transforms infrared spectroscopy (FTIR). XRD was performed using Philips Rigaku Ultima-IV system with CuK_α radiation ($\lambda_{cu} = 1.5418$ Å) within the 2θ range of 5°–65°. TG analyses were performed using a Netzsch TG209 F3 Tarsus thermal analyzer from room temperature to 800 °C at a heating rate of 10 °C min^{-1} under Ar atmosphere. FESEM and FTIR analyses were performed using Nova Nanosem FEI450 operating at 15 kV and Perkin Elmer Spectrum version 10.4.00 in wave number range of 400–4000 cm^{-1} at room temperature, respectively. A drop shape analyzer (Model DSA25, Kruss, Germany) and ImageJ software with preinstalled plug-in were used for CA measurement [43].

3 Results and discussion

3.1 Phase and microstructural analysis

The present approach explores cotton as an effective absorbent for oil/organic solvent removal from water by surface modification and functionalization using rGO by the simple hydrothermal method. The fabrication of rGO@cotton is illustrated in Scheme 1. The pristine cotton was dipped into GO solution and hydrothermally treated using hydrazine hydrate to convert GO into rGO. Thus, we postulate that rGO-anchored cotton (rGO@cotton) was formed due to the weak electrostatic attraction between negatively charged GO species and positively charged hydrogen which transform the hydrophilic cotton to the superhydrophobic surface. XRD of GO synthesized by modified Hummer's method was utilized to investigate the crystalline structure and phase formation as illustrated in Fig. 1a. The diffraction peak of natural graphite powder exists at 26.6° of 2θ value with d-spacing of 0.336 nm [44]. Upon chemical oxidation in the presence of $NaNO_3$ and $KMnO_4$, the Bragg diffraction peak of graphite at 26.6° of 2θ value shift to 11.8° due to increase in the interplanar d-spacing of graphite to 0.74 nm. Here, the increment in the interplanar d-spacing was observed in the case of GO due to oxidation of graphite and the presence of different oxygen functional groups [27]. Figure 1b shows the XRD pattern of rGO, where

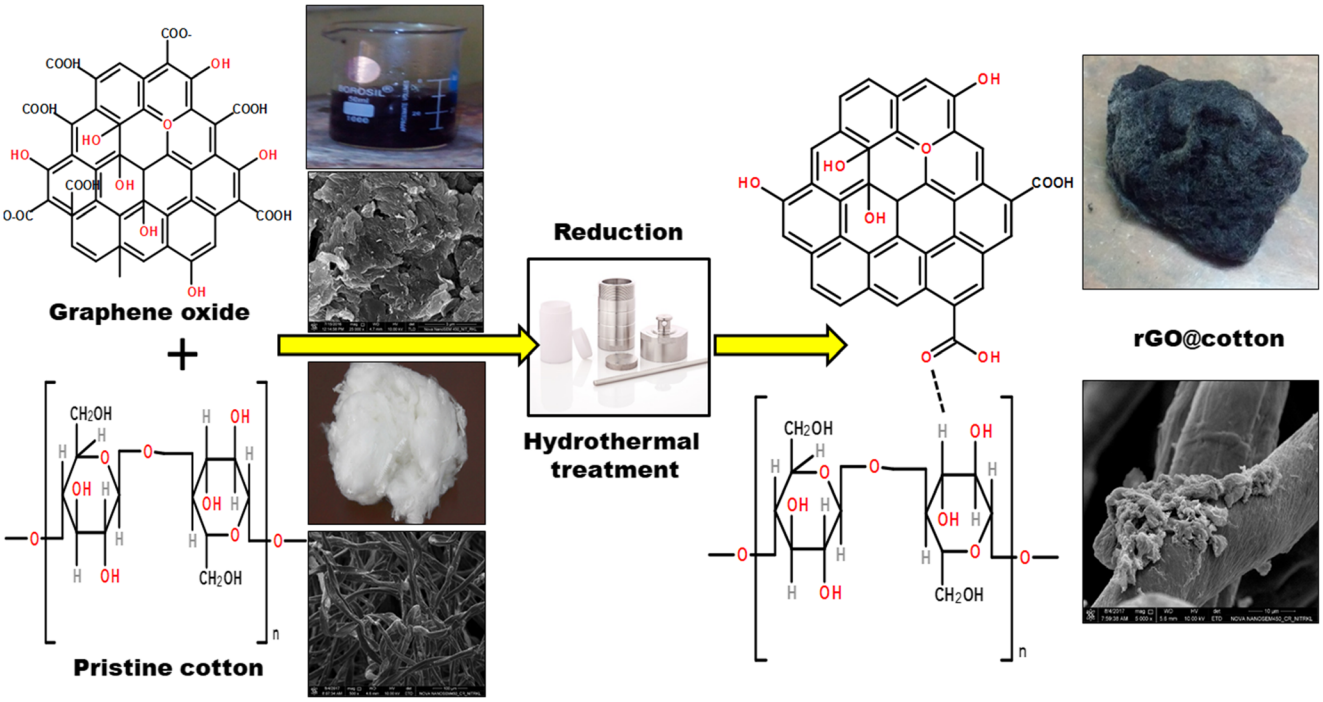

Scheme 1 The proposed mechanism of self-assembly of rGO and pristine cotton during hydrothermal treatment

the hydrothermal treatment of GO has shifted the diffraction peak from 11.8° to 26.6° of 2θ value with a decrease in *d*-spacing value to 0.336 nm due to the removal of oxygen functional groups and restacking of graphene sheets. However, the prepared rGO has a diffraction peak at 26.6° which could be attributed to the graphitic structure (002) of the short-range order in stacked graphene sheets showing a reduction of oxygen bonds [41]. In the XRD profile of pristine cotton, four peaks can be indexed due to the monoclinic structure of cellulose [$(C_6H_{10}O_5)_x$] with Bragg's reflection at 16.62°, 22.4°, 26.6°, and 34.2°, respectively, as shown in Fig. 1c [45]. For rGO@ cotton, the XRD pattern was similar to that of pristine cotton with an additional peak at 26.6° due to the presence of rGO in the cotton (see Fig. 1d). The presence of diffraction peak at 26.6° of 2θ value in the XRD pattern of rGO@cotton also confirms that cotton fibers were completely covered by rGO sheets.

FTIR analysis (see Fig. 2a) shows that the peaks of GO positioned at 3400, 1726, 1622, and 1215 cm^{-1}, respectively, which were attributed to C–OH stretching vibrations, C=O

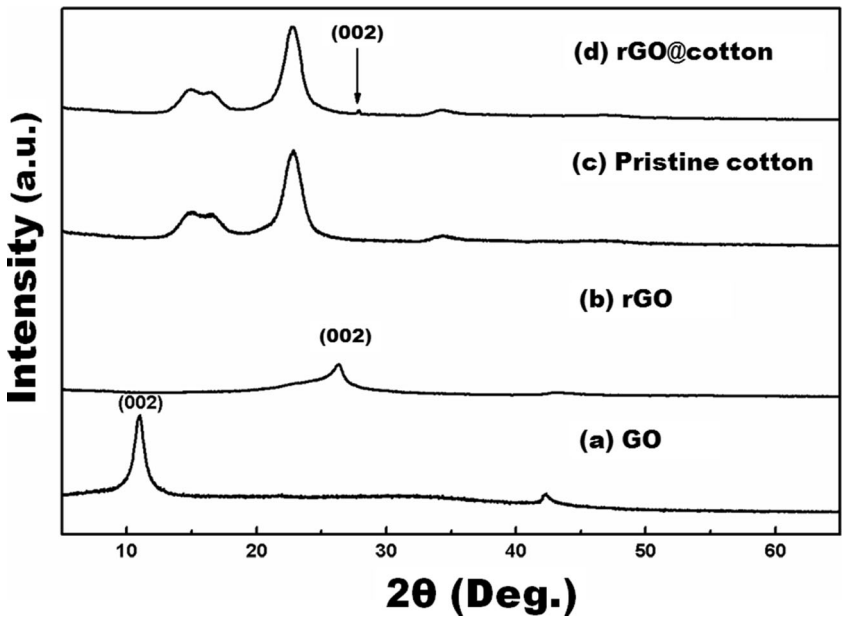

Fig. 1 X-ray diffraction patterns of (a) GO, (b) rGO, (c) pristine cotton, and (d) rGO@cotton

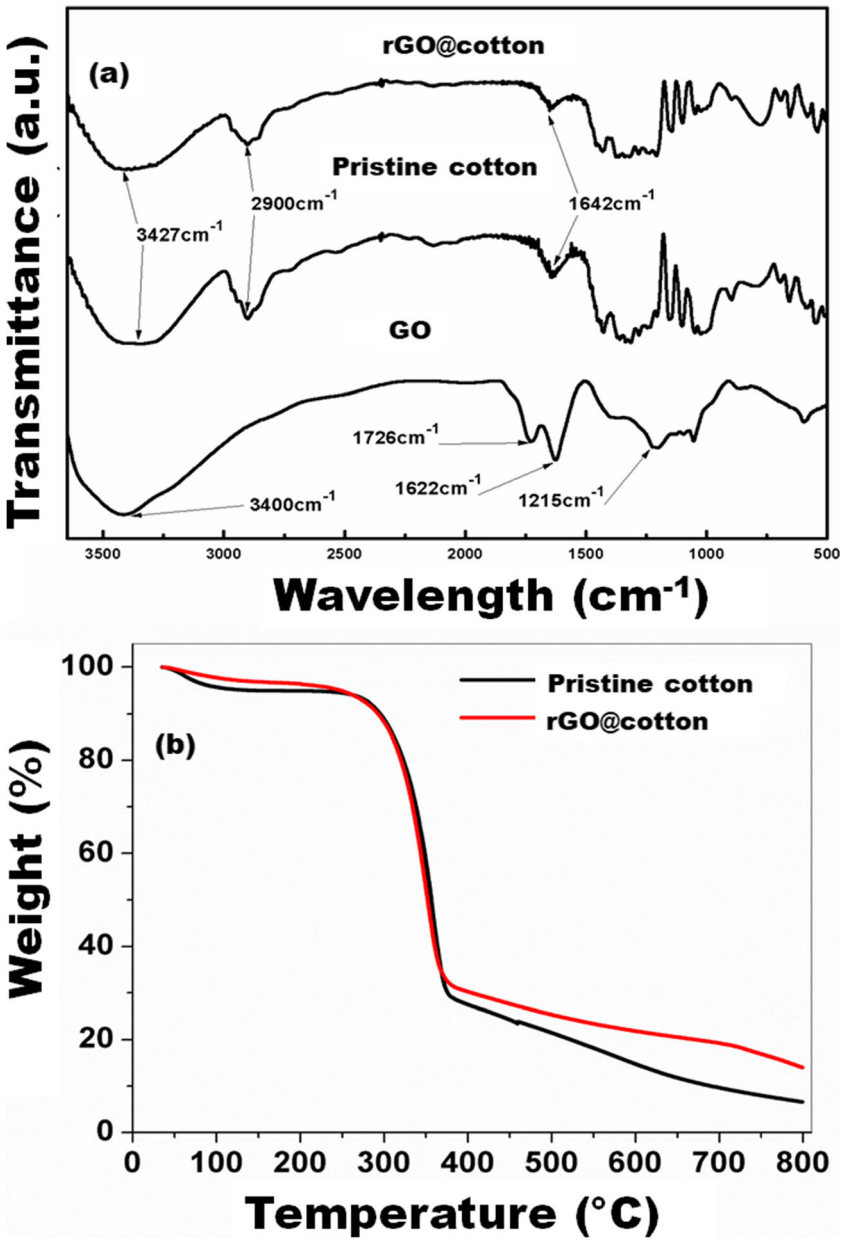

Fig. 2 **a** FTIR spectra of GO, pristine, and rGO@cotton, and **b** TG analysis of pristine and rGO@cotton from room temperature to 800 °C under argon atmosphere

from ketone species and COOH from the carboxylic group, and C–OH stretching for hydroxyl groups [26]. The FTIR pattern of rGO@cotton confirms that hydrothermal treatment indeed resulted in the formation of rGO [42, 44]. The broad absorption peak at 3427 and 2900 cm^{-1} originates due to the stretching vibration of surface −OH and C=O, respectively, whose intensity decreases as compared to that of pristine cotton. Meanwhile, stretching of COOH groups and the functional group present at 1726 and 1215 cm^{-1} was completely absent due to the removal of oxygen group which confirms that GO was reduced into rGO or graphene nanosheets [33]. Moreover, the skeletal vibration appeared at 1642 cm^{-1} was due to absorption band in both pristine and rGO@cotton. Besides, the relative intensity of peaks was decreased in the rGO@cotton as compared to that in pristine cotton in the low-frequency region which confirms the restoration of the aromatic sp^2 hybrid carbon skeleton of graphene [26].

TG analysis was performed to observe the thermal stability of the as-synthesized rGO@cotton and pristine cotton, relatively. Figure 2b shows the mass loss behavior of rGO@cotton and pristine cotton. An identical TG profile with the negligible mass loss was observed up to 250 °C for both pristine cotton and rGO@cotton. However, a rapid mass loss (~70%) within the temperature range of 250 to 300 °C was evident due to thermal decomposition and evaporation of oxygen molecules from the cotton structure [46, 47]. Moreover, ~20% mass loss associated with both pristine cotton and rGO@cotton above 350 to 800 °C is mainly due to the

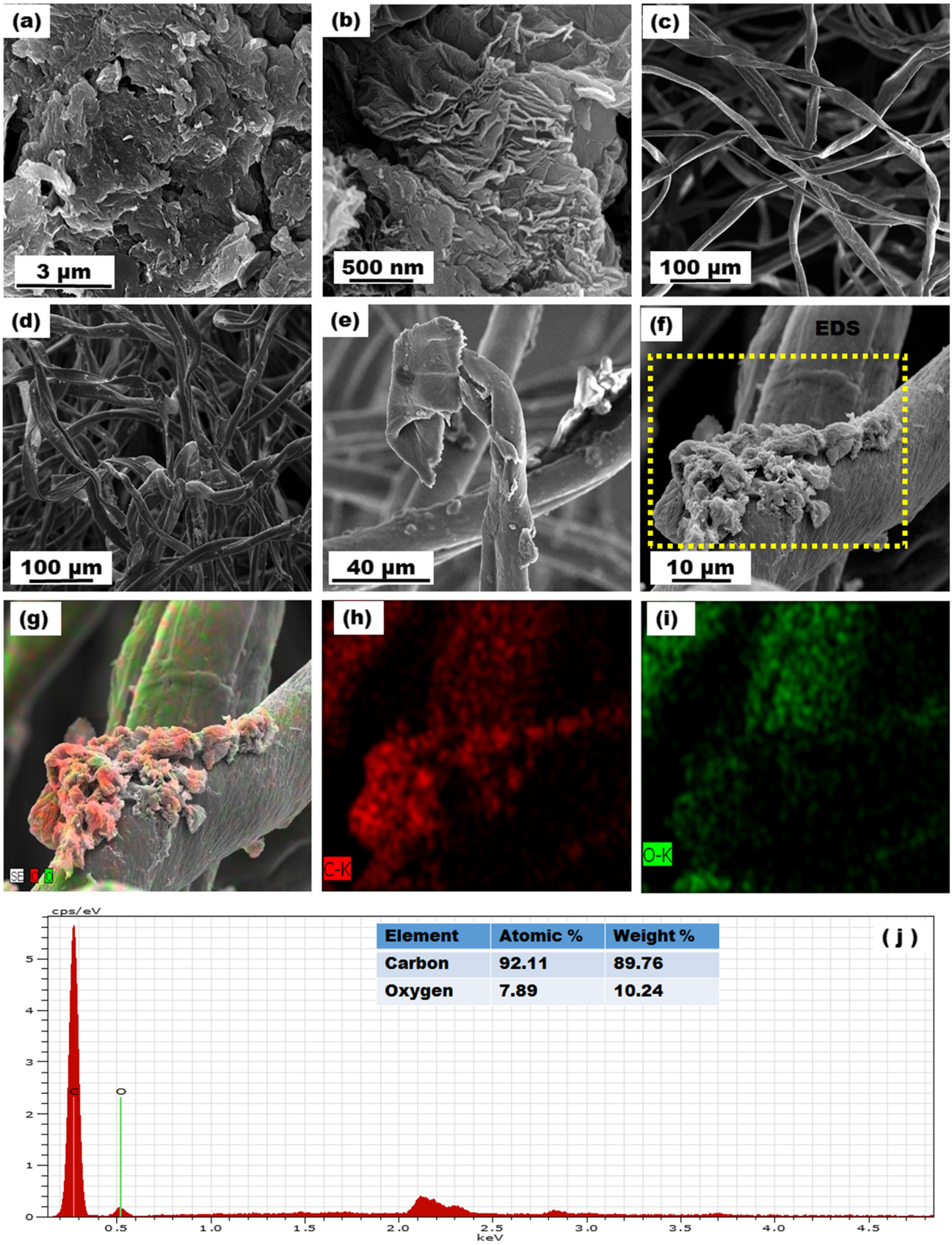

Fig. 3 FESEM images of **a** GO, **b** rGO, and **c**–**f** rGO@cotton; **g**–**i** elemental X-ray mapping showing the elemental distribution of rGO@cotton; and **j** EDS spectra of rGO@cotton

breakdown of the oxygen and hydrogen bonds of the cellulose structure which converted into carbonaceous residues [48]. The similar TG profile for both pristine and rGO@cotton proves that rGO was formed on the cotton surface during hydrothermal treatment, since rGO hardly displays any mass loss behavior during thermal treatment under inert atmosphere [44].

The morphology and microstructure of GO and rGO nanosheets were examined through FESEM analysis. Figure 3a represents the FESEM image of free-standing GO, displaying a rippled and crumpled structure due to exfoliation and restacking processes [49]. FESEM image of the rGO sheets confirmed the restacking of GO occurs in the form of irregular, folded, and wrinkled few layers' sheets (see Fig. 3b). FESEM image of the pristine cotton shows that it has a three-dimensional fibrous network with smooth surface morphology (see Fig. 3c). However, it was apparent that after hydrothermal treatment, the soft cotton fiber was uniformly coated with rGO sheets due to the reduction of GO (see Fig. 3d) [50]. High-magnification FESEM image of the rGO@cotton illustrated in Fig. 3e, f depicts that rGO sheet agglomerated and formed a hierarchical structure. Such a hierarchical structure dramatically increases the surface roughness, and thus, more air can be trapped [33]. However, the roughened surface composed of the micropores is adequate to acquire hydrophobicity and useful during separation of an organic solvent or oil mixed with water. Elemental X-ray mapping of FESEM image (Fig. 3g–i) shows that rGO@cotton contains mainly carbon and oxygen, distributed uniformly. Figure 3j illustrates a full frame EDS spectra of rGO@cotton where the atomic percentage ratio of carbon and oxygen was found ~ 92.11 and 7.89%, respectively, and in good agreement with the nominal composition [33]. Moreover, EDS spectra confirm the presence of thin rGO sheets on the cotton fibers.

3.2 CA measurement

The rGO@cotton derived from the hydrothermal treatment was tested for hydrophobicity and oleophilicity test. Importantly, water droplets kept near-spherical shapes and oil/organic solvents absorbed entirely on the surface of rGO@cotton as shown in Fig. 4a, b. Hydrophobicity and oleophilicity of the rGO@cotton were determined by CA measurement that depends upon CA between a static liquid drop and the solid surface underneath as shown in Fig. 4c. If the CA is less than 90°, then it illustrates the hydrophilic properties of the material as per Young's equation [51]:

$$\mathrm{Cos}\theta = \frac{(\gamma_{sv} - \gamma_{sl})}{\gamma_{lv}}$$

where γ_{sl}, γ_{sv}, and γ_{lv} are the interfacial free energies per unit area of the solid-liquid, solid-vapor, and liquid-vapor interfaces, respectively. However, if the contact angle is greater than 90° and 150°, that demonstrates hydrophobic and superhydrophobic properties of the material, respectively [52–54]. The CA of water-in-air on rGO@cotton was measured ~ 162.9° by the drop shape analyzer, and ImageJ software (inset) suggests the formation of superhydrophobic surface (see Fig. 4c). Also, it was evident that air bubbles got trapped at the bottom of the water droplet to avoid absorption, which suggests the formation of a non-wetting Cassie-Baxter

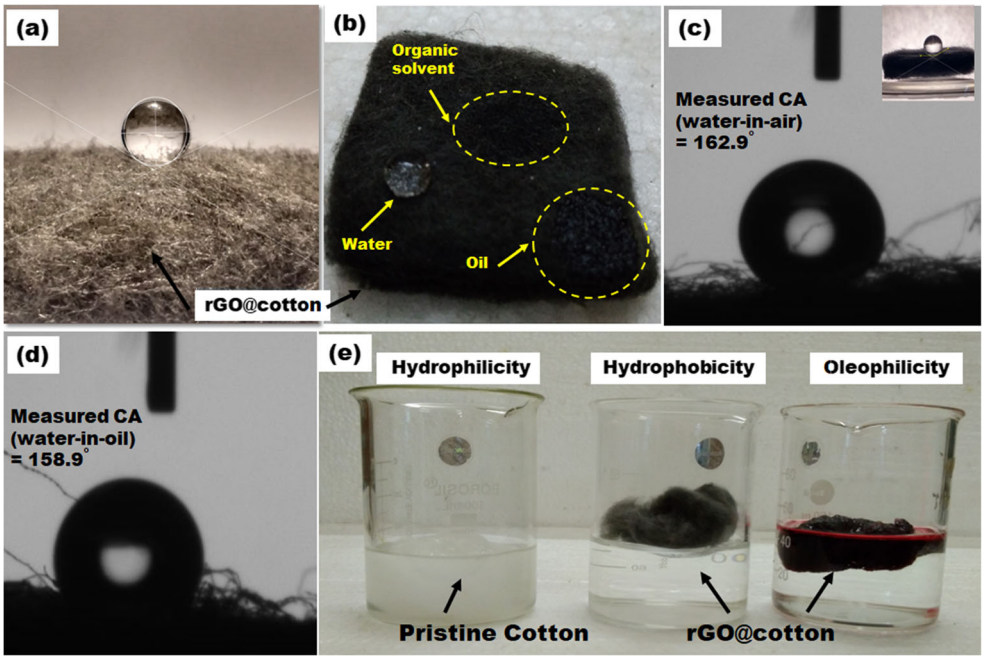

Fig. 4 Digital images of **a** water droplet; **b** a static water drop and absorbed oil/organic solvents drop; **c** CA measurement of static water droplet, using Drop Size Analyzer and ImageJ software (inset); **d** CA measurement of static water droplet on pre-oil-wetted rGO@cotton; **e** hydrophilicity, hydrophobicity, and oleophilicity of pristine cotton and rGO@cotton, respectively, towards oil-water mixture

surface on the rGO@cotton [39]. Moreover, the CA of water-in-oil on rGO@cotton was measured ~ 158.9° by placing a water droplet as the probe on the pre-oil-wetted rGO@cotton surface as shown in Fig. 4d. The as-synthesized rGO@cotton displayed superhydrophilic behavior for oil/organic solvents by rapidly absorbing oil and organic solvents, which suggested the 0° CA of oil or organic solvents-in-air on the rGO@cotton (see Fig. 4b). However, it is to be noted that rGO@cotton surface exhibited hydrophilic behavior for water on pre organic solvents-wetted rGO@cotton surface because superhydrophobicity of the sorbent weakened after it was wetted with organic solvent before the onset of separation test. The hydrophobicity and oleophilicity of the rGO@cotton are evident in a series of photographs depicted in Fig. 4e. The pristine cotton is hydrophilic as it gets completely submerged in water; however, the rGO@cotton floats and remains stable in water and absorbs oil entirely due to its hydrophobic and oleophilic nature, respectively (see Fig. 4e and Video 1 in electronic supplementary information). The primary reason for superhydrophobicity, superoleophilicity, and high selectivity of modified rGO@cotton is equal surface energies between rGO@cotton and oils [55]. It is worthy to note that rGO@cotton absorbs oil or different organic solvent entirely and thoroughly wets the surface due to close surface energies between rGO@cotton (~ 46.7 mJ/m^2) and oil (~ 31.6 mJ/m^2) [54]. However, rGO@cotton shows superhydrophobicity with water due to a significant difference in surface energies between rGO@cotton (~ 46.7 mJ/m^2) and water (~ 72 mJ/m^2) [56].

3.3 Absorption capacity

To calculate the absorption capacity, a mixed solution of oil/organic solvent with water with a volumetric ratio of 1:4 was filled in a 100-ml beaker. To get the accurate results, the experiment was repeated ten times using the 200 mg equal weight of rGO@cotton. It was observed that rGO@cotton rapidly soaked the oil/organic solvent within 30 s when placed in the solution mixture. However, rGO@cotton did not interact with the water due to hydrophobicity as mentioned earlier. Moreover, the increment of the initial weight of rGO@cotton and decrement in the total volume of the solution after first cycle absorption test confirm the oleophilicity and hydrophobicity of the synthesized product. Interestingly, absorption capacities of rGO@cotton depend on the viscosity and density of different organic solvents and oils. Oil-loaded rGO@cotton was collected on a petri dish which shows that substantial volume of oil was absorbed from the mixture. Similarly, organic solvents (dyed with oil red IV) soaked into rGO@cotton was also collected in petri dishes, which showed a decrease in total volume and level in the beaker confirms the removal of organic solvent from the water (see Video 2 in electronic supplementary information). Importantly, oils and organic solvents can be easily collected by mechanically squeezing the rGO@cotton and reused for further absorption test.

We also investigated the maximum rGO loading on the cotton which requires for obtaining the maximum oil absorption capacity by varying the concentration of GO during rGO@cotton synthesis. Figure 5a illustrates the absorption capacity of engine oil with various rGO loadings. It was found that with increasing GO concentration from 0.5 to 1.5 mg/ml, absorption capacity increases, but above 1.5 mg/ml GO level, there was a decrease in absorption capacity. Moreover, absorption capacity of ~ 46.54, ~ 51.83, ~ 57.01, ~ 51.49, and ~ 45.9 g/g was observed for the concentration of 0.5, 1, 1.5, 2, and 2.5 mg/ml of rGO@cotton after 0 min, respectively (see Fig. 5b). Therefore, it was apparent that maximum absorption capacity was achieved with 1.5 mg/ml rGO@cotton compares to other rGO loading even after 15-min time interval or after 24–48 h. To understand the absorption capacity of rGO@cotton, various oils and organic solvents were selected, including engine oil, pump oil, acetone, propanol, DMF, and NMP. In a typical oil-water separation experiment, an rGO@cotton was dipped in engine oil mixed with water as shown in Fig. 5c–f and within a few seconds, the oil was absorbed completely by the rGO@cotton without absorbing any water. Superoleophilicity of rGO@cotton depends on the open pores that exist in the cotton because oil can permeates through the channel by a capillary force, resulting in higher wettability of rGO@cotton by oil. However, water remains on the surface of rGO@cotton due to superhydrophobicity. The absorption capacity was determined by mass gain or the ratio of the absorbed oil mass to the as-prepared rGO@cotton, defined as gram per gram. The as-prepared rGO@cotton displayed excellent absorption capacities ranging from ~40 to 55 times of its weight for a variety of oils and organic solvents (see Fig. 5g and Video 3 in electronic supplementary information). The absorption efficiency for rGO@cotton was much higher than that for various sorbents hitherto reported in the literature [26–29]. However, it was noticed that rGO@cotton releases oil/organic solvent with time if placed in a petri dish. It was found that absorption capacity decreased from ~ 33 to ~ 24.3% of engine oil within 60 min. A similar trend was also noticed for other oils mainly due to surface tension force that develops between the oil and the petri dish which helps the oil to release from the sorbent with time. The maximum difference in absorption capacity was observed in the case of pump oil and acetone. Since acetone has a low boiling point (~ 56 °C), it may be possible that partial mass loss originated due to volatilization (see Fig. 5h).

3.4 A kinetic model for sorption mechanism

To investigate the absorption behavior of rGO@cotton, the absorption capacity and sorption mechanism of oil and

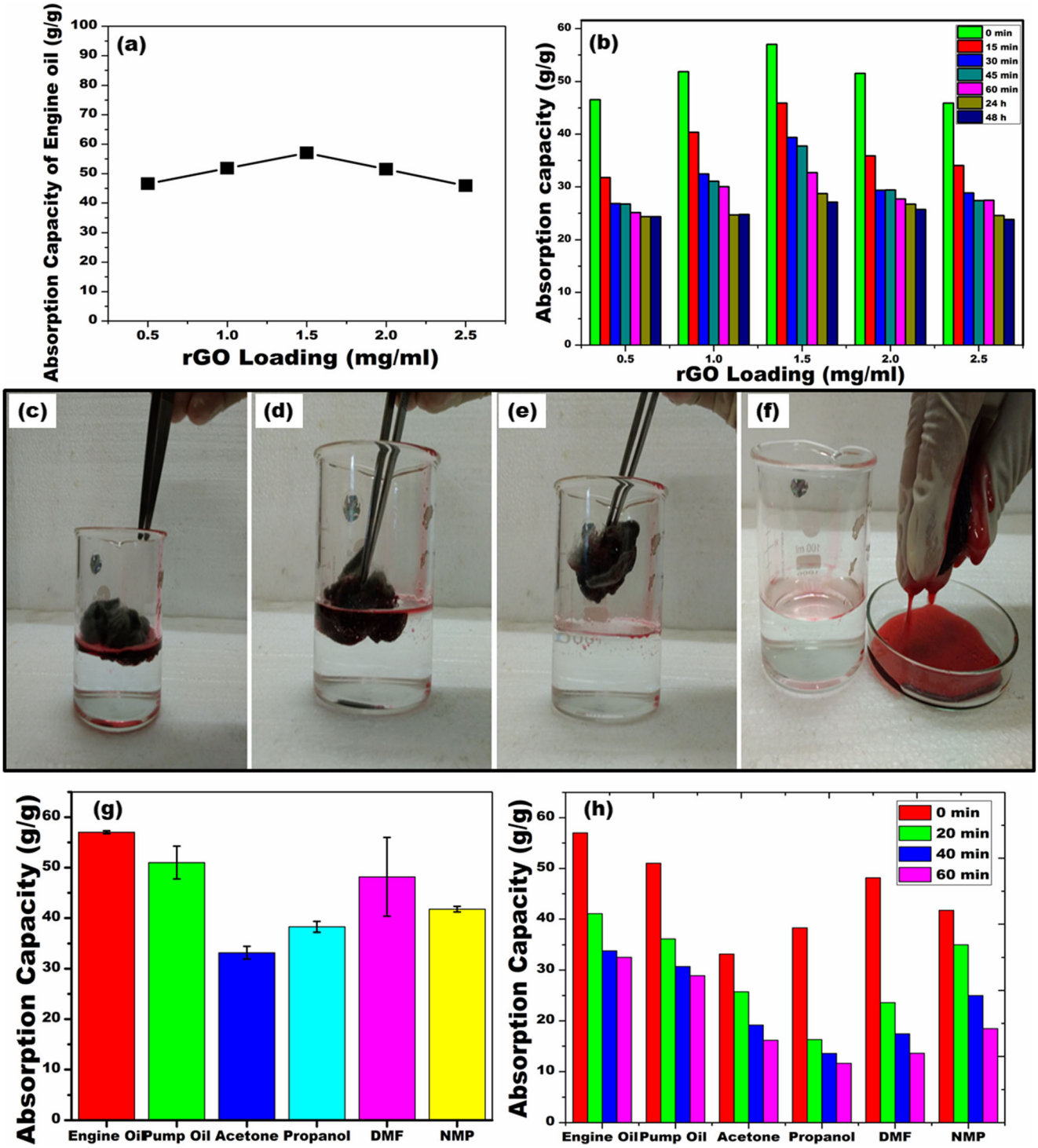

Fig. 5 **a** Variation of absorption capacity with rGO loading for engine oil, **b** variation of absorption capacity with rGO loading at different holding time for engine oil, **c**–**f** digital images showing oil-water separation test, **g** absorption capacity of oils and organic solvents by rGO@cotton at the first cycle, **h** absorption capacity of oils and organic solvents by rGO@cotton at the first cycle with different holding time

organic solvent were studied using pseudo-second-order kinetic equation as given below [57–59]:

$$\frac{1}{Q_s - Q_t} - \frac{1}{Q_s} = K.t$$

where Q_s indicates the saturated sorption capacity, Q_t is the amount of sorption at time t, t represents the sorption time, and K is the sorption constant which is viscosity-dependent. rGO@cotton possesses an interconnected highly porous structure that rapidly absorbs oil and organic solvents with time.

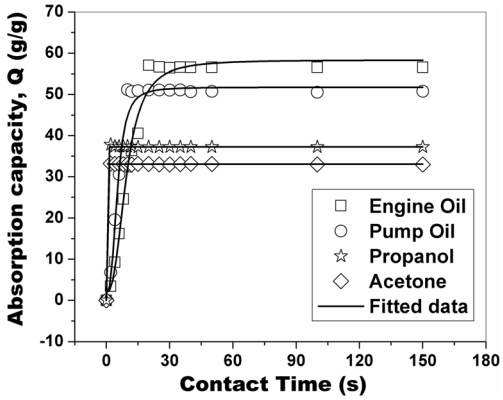

Fig. 6 Sorption kinetics behavior of rGO@cotton with time for engine oil, pump oil, acetone, and propanol

However, sorption characteristics of oil and organic solvents depend not only on porosity but also on the viscosity of the oil. Kinetics behavior of rGO@cotton for various oils is shown in Fig. 6. It is apparent that absorption behavior of high viscous engine oil and pump oil takes longer time compared to low viscous acetone and propanol. The absorption capacity of low viscous acetone and propanol reached to saturated absorption capacity (Q_s) within 1 s but sorption of high viscous oil took more than 20–30 s to reach the saturated capacity. Interestingly, low viscous solvents penetrate rapidly inside the interconnected porous structure of rGO@cotton due to the faster diffusion process. However, high viscosity oil retains on the surface and diffusion into the pore takes longer time.

Saturated sorption capacity (Q_s), sorption constant (K), and saturation time (t_s) were calculated using pseudo-second-order kinetics equation and summarized in Table 1. The experimental data were fitted with the pseudo-second-order kinetic model (see Fig. 6) and excellent agreement was achieved with R^2 value greater than 0.95. For engine oil/water separation process, rGO@cotton exhibits a slightly low sorption rate with K value of ~ 0.11 s^{-1}. On the contrary, pump oil, acetone, and propanol/water separation showed relatively higher K value of ~ 0.48, ~ 0.80, and ~ 0.55 s^{-1}, respectively. However, relatively higher K value of pump oil, acetone, and propanol compare to that of engine oil is due to fast absorption of pump oil, acetone, and propanol by rGO@cotton as mentioned due to viscosity difference. The above results validate that the sorption kinetics of oil and organic solvents depends not only on sorbent structure but also on the viscosity of oil or organic solvents which effectively accelerate or decelerate the absorption kinetics.

We also found the CA and absorption capacity remain stable with temperature for superhydrophobic/superoleophilic rGO@cotton as shown in Fig. 7a. The CA of water-in-air remains constant around ~ 155° from room temperature up to 150 °C. It was noticed that absorption capacity increases slightly (~ 1.03 g/g) with 30 °C increases in temperature (see Fig. 7b). The above results confirm that rGO@cotton can withstand high temperature and potentially be used during oil spill burning. However, it may be possible that with increasing temperature, the surface becomes hydrophilic due to a decrease in surface tension of rGO@cotton [60].

3.5 Reusability

The reusability plays a major role in oil spill clean-up for any practical sorbents. The absorption capacity (AC) and collection capacity (CC) for various oils/organic solvents were determined for ten cycles [see Fig. 8a]. It was found that rGO@cotton can absorb ~ 57.01, ~ 53.5, ~ 33.17, ~ 38.27, ~ 48.2, and ~ 41.7 g/g of engine oil, pump oil, acetone, propanol, DMF, and NMP for zero cycle, respectively. However, AC decreases after the first cycle and remains constant for the tenth cycle due to the presence of oil/solvent residue after mechanical squeezing. The rGO-coated cotton after the first cycle can absorb ~ 38 and ~ 37 g/g of engine oil and pump oil, respectively, which remains as ~ 21 and ~ 25 g/g the at tenth cycle (see Fig. 8a). Table 2 shows the AC and CC retentions from the first cycle to tenth cycle of rGO@cotton for different oil and organic solvents. It is true that rGO@cotton exhibited excellent AC from ~ 41 to 57 g/g for engine oil, pump oil, acetone, propanol, NMP, and DMF. Moreover, rGO@cotton showed good agreement for recyclability application with AC retention ~ 40–60% and ~ 30–35% for the fifth cycle and tenth cycle, respectively. Importantly, CC was always maintained in the scope of ~ 0.2 g/g after each cycle validates the potential for reusability of rGO@cotton. The slight fall in AC was mainly due to the presence of different amounts of residual oils and organic solvent in squeezed cotton, which cannot be desorbed completely without drying. It is also possible that AC for low molecular weight solvents such as acetone, propanol, NMP, and DMF

Table 1 Density, viscosity for oils and organic solvents and calculated parameter(s) obtained from the second-order kinetic equation

Reagent	Density (g/ml)	Viscosity (mPa s)	K (s^{-1})	Q_s (g/g)	t_s (s)	R^2
Engine oil	0.87	155.31	0.11	57.02	20	0.98
Pump oil	0.86	204.00	0.48	51.18	10	0.96
Acetone	0.78	0.31	0.80	33.20	1	0.99
Propanol	0.80	2.05	0.55	37.83	1	0.99

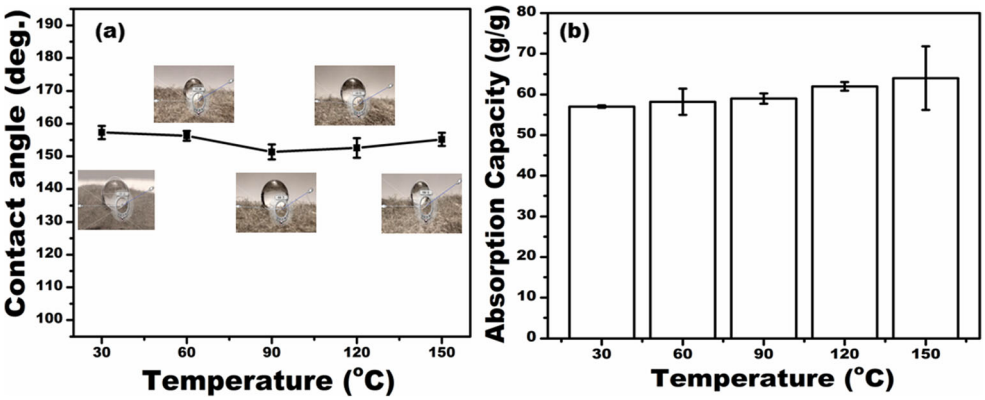

Fig. 7 Variation of **a** contact angle and **b** absorption capacity with temperature

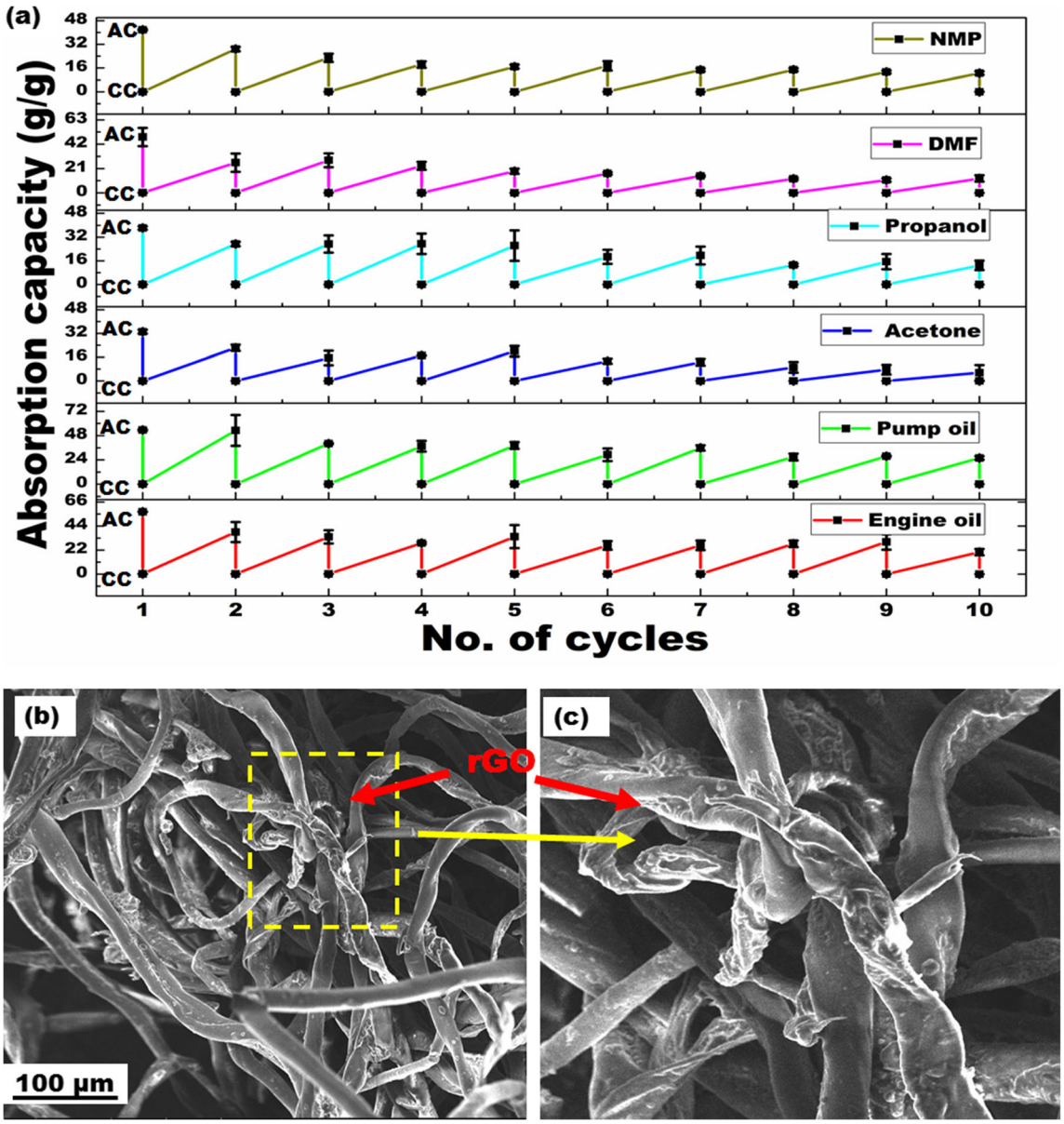

Fig. 8 **a** Variation of absorption capacity and collection capacity of oils and different organic solvents up to ten cycles, **b**–**c** FESEM images of rGO@cotton after ten cycles sorption-mechanical squeezing test

Table 2 Absorption capacities and collection capacities of rGO@cotton-based material with various oils and organic solvents after the fifth and tenth cycle sorption-mechanical squeezing test

Oil and organic solvents	AC at 1st cycle (g/g)	CC at 1st cycle (g/g)	AC retention after 5th cycle (%)	CC variation after 5th cycle (g/g)	AC retention after 10th cycle (%)	CC variation after 10th cycle (g/g)
Engine oil	57.02	0.10	60.09	0.03	35.17	0.03
Pump oil	51.10	0.04	74.88	0.08	50.67	0.08
Acetone	33.20	0.06	60.40	0.06	16.90	0.06
Propanol	37.83	0.05	70.40	0.07	34.21	0.07
DMF	48.17	0.10	38.62	0.06	25.81	0.06
NMP	41.74	0.07	40.30	0.02	30.00	0.02

remained constant up to ten cycles due to low viscosity nature of those solvents. However, only ~35–40% oils can only be recovered by mechanical squeezing due to high viscous nature of the oils used here. FESEM analysis of recycled rGO@cotton revealed a highly stable bond between rGO and cotton fibers, which suggests the mechanical robustness of the synthesized product after absorption/desorption test up to ten cycles (see Fig. 8b–e). Importantly, stable AC from the first to tenth cycle suggests the efficacy of rGO@cotton for practical oil spill clean-up. Table 3 shows a similar data of absorption capacity of various sorbents hitherto reported in the literature with as-synthesized rGO@cotton. It is worthy to mention that rGO@cotton showed excellent absorption capacity for engine oil, pump oil, acetone, propanol, DMF, and NMP compare to previously reported data found in the literature. The sorption capacity of rGO@cotton is comparable to that of robust and durable cotton fabrics [40], flower-like TiO_2@cotton [61], and superhydrophobic cotton [6].

4 Conclusions

In the present work, rGO@cotton was synthesized by hydrothermal method using GO, cotton ball, and hydrazine hydrate

Table 3 Comparison of oil and organic solvent absorption behavior of rGO- and cotton-based materials synthesized by different routes

Absorbent materials	Synthesis route	Absorption type	Capacity	References
Superhydrophobic cotton	SiO_2 nanoparticles modification	Oil	50 times of its weight	[6]
rGO-coated cottons	Dip coating of polydimethylsiloxane	Organic solvents and oils	11 to 25 times its weight	[23]
Robust and durable cotton fabrics	Chemical modification by polyaniline (PANI)	Oil	97.8% of their weight	[40]
rGO membranes	Polydopamine-coated rGO	Oil-in-water emulsion	outstanding separation efficiency	[31]
Graphene-coated cotton	Hydrothermal method	Oil	30 times its weight	[33]
Multifunctional rGO-coated cloths	Thermal treatment	Oil and antibacterial application	98%	[34]
rGO cotton	Thermal reduction	Oil	22–45 times its weight	[45]
Flower-like TiO_2 @cotton	Hydrothermal method	Oil	99.8%	[61]
Graphene oxide modified Al_2O_3 membrane	Solution immersion	Oil-water separation	Higher oil rejection	[62]
Superhydrophobic fabrics	Plasma-enhanced chemical vapor deposition	Oil-water separation	Higher water rejection	[63]
Superhydrophobic fiberglass cloth	Silane modification	Oil-water separation	98% separation efficiency	[64]
Graphene-wrapped sponge	Centrifugation-assisted dip coating	Oil recovery	94.6%	[35]
Superhydrophobic cotton fabrics	Polydimethylsiloxane and ZnO coating	Oil-water separation	Higher water rejection	[65]
Hydrophobic-reduced graphene oxide	Hydrothermal method	Oil-water separation	Excellent separation efficiency	[29]
rGO@cotton (reduced graphene oxide-coated cotton)	Hydrothermal method	Engine oil Pump oil acetone Propanol DMF NMP	57.01 g/g 53.50 g/g 33.17 g/g 38.27 g/g 48.20 g/g 41.70 g/g	Present work

as reducing agents. rGO@cotton exhibited CA of water-in-air ~ 162.9° that confirms the superhydrophobicity of the surface. Also, synthesized rGO@cotton showed excellent oil-water separation behavior such as high selectivity, good absorption efficiency, and excellent recyclability. It was observed that rGO@cotton can separate 40–60 times oils/solvents of its weight from water. Therefore, it can be concluded that modified rGO@cotton will be a promising alternative for the conventional sorbents used in the large-scale oil spill clean-up from the oil-water mixture.

Acknowledgements Authors gratefully acknowledge the partial financial support from the Department of Science and Technology, Science and Engineering Research Board (DST-SERB) (grant number ECR/2016/000959).

Compliance with ethical standards

Conflict of interest The authors declare that they have no conflict of interest.

References

1. Chu Z, Feng Y, Seeger S (2015) Oil/Water Separation with Selective Superantiwetting/Superwetting Surface Materials. Angew Chem Int Ed 54:2328. https://doi.org/10.1002/anie.201405785
2. Ma Q, Cheng H, Fane AG, Wang R, Zhang H (2016) Recent Development of Advanced Materials with Special Wettability for Selective Oil/Water Separation. Small 12:2186. https://doi.org/10.1002/smll.201503685
3. Chen P-C, Xu Z-K (2013) Mineral-Coated Polymer Membranes with Superhydrophilicity and Underwater Superoleophobicity for Effective Oil/Water Separation. Sci Rep 3:2776. https://doi.org/10.1038/srep02776
4. Gupta RK, Dunderdale GJ, England MW, Hozumi A (2017) Oil/water separation techniques: a review of recent progresses and future directions. J Mater Chem A 5:16025-58. https://doi.org/10.1039/C7TA02070H
5. Kota AK, Kwon G, Choi W, Mabry JM, Tuteja A (2012) Hygro-responsive membranes for effective oil-water separation. 3:1025. https://doi.org/10.1038/ncomms2027
6. Liu F, Ma M, Zang D, Gao Z, Wang C (2014) Fabrication of superhydrophobic/superoleophilic cotton for application in the field of water/oil separation. Carbohydr Polym 103:480. https://doi.org/10.1016/j.carbpol.2013.12.022
7. Li R, Chen C, Li J, Xu L, Xiao G, Yan D (2014) A facile approach to superhydrophobic and superoleophilic graphene/polymer aerogels. J Mater Chem A 2:3057. https://doi.org/10.1039/C3TA14262K
8. Zhu Q, Pan Q, Liu F (2011) Facile Removal and Collection of Oils from Water Surfaces through Superhydrophobic and Superoleophilic Sponges. J Phys Chem C 115:17464. https://doi.org/10.1021/jp2043027
9. Gupta S, Tai N-H (2016) Carbon materials as oil sorbents: a review on the synthesis and performance. J Mater Chem A 4:1550. https://doi.org/10.1039/C5TA08321D
10. Inagaki M, Konno H, Toyoda M, Moriya K, Kihara T (2000) Sorption and recovery of heavy oils by using exfoliated graphite Part II: Recovery of heavy oil and recycling of exfoliated graphite. Desalination 128:213. https://doi.org/10.1016/S0011-9164(00)00035-7
11. Li H, Zhao X, Wu P, Zhang S, Geng B (2016) Facile preparation of superhydrophobic and superoleophilic porous polymer membranes for oil/water separation from a polyarylester polydimethylsiloxane block copolymer. J Mater Sci 51:3211. https://doi.org/10.1007/s10853-015-9632-6
12. Yu Y, Wu X, Fang J (2015) Superhydrophobic and superoleophilic "sponge-like" aerogels for oil/water separation. J Mater Sci 50:5115. https://doi.org/10.1007/s1085
13. Wang Y, Liu X, Lian M et al (2017) Continuous fabrication of polymer microfiber bundles with interconnected microchannels for oil/water separation. Appl Mater Today 9:77. https://doi.org/10.1016/j.apmt.2017.05.007
14. Dunderdale GJ, Urata C, Sato T, England MW, Hozumi A (2015) Continuous, high-speed, and efficient oil/water separation using meshes with antagonistic wetting properties. ACS Appl Mater Interfaces 7:18915. https://doi.org/10.1021/acsami.5b06207
15. Yin K, Chu D, Dong X, Wang C, Duan J-A, He J (2017) Femtosecond laser-induced robust periodic nanoripple structured mesh for highly efficient oil-water separation. Nano 9:14229. https://doi.org/10.1039/C7NR04582D
16. Bi H, Yin Z, Cao X et al (2013) Carbon fiber aerogel made from raw cotton: a novel, efficient and recyclable sorbent for oils and organic solvents. Adv Mater 25:5916. https://doi.org/10.1002/adma.201302435
17. Liu Q, Patel AA, Liu L (2014) Superhydrophilic and underwater superoleophobic poly (sulfobetaine methacrylate)-grafted glass fiber filters for oil-water separation. ACS Appl Mater Interfaces 6:8996. https://doi.org/10.1021/am502302g
18. Gui X, Wei J, Wang K et al (2010) Carbon Nanotube Sponges. Adv Mater 22:617. https://doi.org/10.1002/adma.200902986
19. Sansotera M, Navarrini W, Resnati G et al (2010) Preparation and characterization of superhydrophobic conductive fluorinated carbon blacks. Carbon 48:4382. https://doi.org/10.1016/j.carbon.2010.07.052
20. Zhao M, Liu P (2009) Adsorption of methylene blue from aqueous solutions by modified expanded graphite powder. Desalination 249:331. https://doi.org/10.1016/j.desal.2009.01.037
21. Ren H, Shi X, Zhu J, Zhang Y, Bi Y, Zhang L (2016) Facile synthesis of N-doped graphene aerogel and its application for organic solvent adsorption. J Mater Sci 51:6419. https://doi.org/10.1007/s10853-016-9939-y
22. Araby S, Qiu A, Wang R, Zhao Z, Wang C-H, Ma J (2016) Aerogels based on carbon nanomaterials. J Mater Sci 51:9157. https://doi.org/10.1007/s10853-016-0141-z
23. Sun H, Zhu Z, Liang W et al (2014) Reduced graphene oxide-coated cotton for selective absorption of organic solvents and oils from water. RSC Adv 4:30587. https://doi.org/10.1039/C4RA03208J
24. Xiao N, Zhou Y, Ling Z, Qiu J (2013) Synthesis of a carbon nanofiber/carbon foam composite from coal liquefaction residue for the separation of oil and water. Carbon 59:530. https://doi.org/10.1016/j.carbon.2013.03.051
25. Sun Z, James DK, Tour JM (2011) Graphene chemistry: synthesis and manipulation. J Phys Chem Lett 2:2425. https://doi.org/10.1021/jz201000a
26. Singh V, Joung D, Zhai L, Das S, Khondaker SI, Seal S (2011) Graphene based materials: past, present and future. Prog Mater Sci 56:1178. https://doi.org/10.1016/j.pmatsci.2011.03.003
27. Zaaba NI, Foo KL, Hashim U, Tan SJ, Liu W-W, Voon CH (2017) Synthesis of Graphene Oxide using Modified Hummers Method: Solvent Influence. Procedia Eng 184:469. https://doi.org/10.1016/j.proeng.2017.04.118
28. Hummers WS, Offeman RE (1958) Preparation of Graphitic Oxide. J Am Chem Soc 80:1339. https://doi.org/10.1021/ja01539a017
29. Tang Z, Zhang Z, Han Z, Shen S, Li J, Yang J (2016) One-step synthesis of hydrophobic-reduced graphene oxide and its oil/water

separation performance. J Mater Sci 51:8791. https://doi.org/10.1007/s10853-016-9937-0
30. Fragouli D, Athanassiou A (2017) Graphene heaters absorb faster. Nature Nano 12:406. https://doi.org/10.1038/nnano.2017.63
31. Liu N, Zhang M, Zhang W et al (2015) Ultralight free-standing reduced graphene oxide membranes for oil-in-water emulsion separation. J Mater Chem A 3:20113. https://doi.org/10.1039/C5TA06314K
32. Liu Y, Ma J, Wu T et al (2013) Cost-effective reduced graphene oxide-coated polyurethane sponge as a highly efficient and reusable oil-absorbent. ACS Appl Mater Interfaces 5:10018. https://doi.org/10.1021/am4024252
33. Ge B, Zhang Z, Zhu X, Men X, Zhou X, Xue Q (2014) A graphene coated cotton for oil/water separation. Compos Sci Technol 102:100. https://doi.org/10.1016/j.compscitech.2014.07.020
34. Upadhyay RK, Dubey A, Waghmare PR, Priyadarshini R, Roy SS (2016) Multifunctional reduced graphene oxide coated cloths for oil/water separation and antibacterial application. RSC Adv 6:62760. https://doi.org/10.1039/C6RA08079K
35. Ge J, Shi L-A, Wang Y-C et al (2017) Joule-heated graphene-wrapped sponge enables fast clean-up of viscous crude-oil spill. Nat Nanotechnol 12:434. https://doi.org/10.1038/nnano.2017.33
36. Periasamy AP, Wu W-P, Ravindranath R, Roy P, Lin G-L, Chang H-T (2017) Polymer/reduced graphene oxide functionalized sponges as superabsorbents for oil removal and recovery. Mar Pollut Bull 114:888. https://doi.org/10.1016/j.marpolbul.2016.11.005
37. Luo Y, Jiang S, Xiao Q, Chen C, Li B (2017) Highly reusable and superhydrophobic spongy graphene aerogels for efficient oil/water separation. Sci Rep 7:7162. https://doi.org/10.1038/s41598-017-07583-0
38. Niu Z, Chen J, Hng HH, Ma J, Chen X (2012) A leavening strategy to prepare reduced graphene oxide foams. Adv Mater 24:4144. https://doi.org/10.1002/adma.201200197
39. Zhang M, Wang C, Wang S, Li J (2013) Fabrication of superhydrophobic cotton textiles for water-oil separation based on drop-coating route. Carbohydr Polym 97:59. https://doi.org/10.1016/j.carbpol.2012.08.118
40. Zhou X, Zhang Z, Xu X et al (2013) Robust and durable superhydrophobic cotton fabrics for oil/water separation. ACS Appl Mater Interfaces 5:7208. https://doi.org/10.1021/am4015346
41. Shahriary L, Athawale AA (2014) Graphene oxide synthesized by using modified hummers approach. Int J Renew Energy Environ Eng 2:58. https://doi.org/10.1016/j.proeng.2017.04.118
42. Nethravathi C, Rajamathi M (2008) Chemically modified graphene sheets produced by the solvothermal reduction of colloidal dispersions of graphite oxide. Carbon 46:1994. https://doi.org/10.1016/j.carbon.2008.08.013
43. Lamour G, Hamraoui A, Buvailo A et al (2010) Contact angle measurements using a simplified experimental setup. J Chem Educ 87:1403. https://doi.org/10.1021/ed100468u
44. Abdolhosseinzadeh S, Asgharzadeh H, Seop Kim H (2015) Fast and fully-scalable synthesis of reduced graphene oxide. Sci Rep 5:10160. https://doi.org/10.1038/srep10160
45. Hoai NT, Sang NN, Hoang TD (2017) Thermal reduction of graphene-oxide-coated cotton for oil and organic solvent removal. Mater Sci Eng B 216:10. https://doi.org/10.1016/j.mseb.2016.06.007
46. Leng B, Shao Z, de With G, Ming W (2009) Superoleophobic cotton textiles. Langmuir 25:2456. https://doi.org/10.1021/la8031144
47. Zhu H, Yang S, Chen D, et al (2016) A Robust Absorbent Material Based on Light-Responsive Superhydrophobic Melamine Sponge for Oil Recovery. Adv Mater Interfaces 3:1500683. https://doi.org/10.1002/admi.201500683
48. Richard-Campisi L, Bourbigot S, Le Bras M, Delobel R (1996) Thermal behaviour of cotton-modacrylic fibre blends: kinetic study using the invariant kinetic parameters method. Thermochim Acta 275:37. https://doi.org/10.1016/0040-6031(95)02729-7
49. Shalaby A, Nihtianova D, Markov P, Staneva A, Iordanova R, Dimitriev Y (2015) Structural analysis of reduced graphene oxide by transmission electron microscopy. Bulg Chem Commun 47:291
50. Bong J, Lim T, Seo K et al (2015) Dynamic graphene filters for selective gas-water-oil separation. Sci Rep 5:14321. https://doi.org/10.1038/srep14321
51. Nakajima A, Hashimoto K, Watanabe T (2001) Recent studies on super-hydrophobic films. Monatshefte für Chemie Chem Month 132:31. https://doi.org/10.1007/s007060170142
52. Kubiak K, Wilson M, Mathia T, Carval P (2011) Wettability versus roughness of engineering surfaces. Wear 271:523. https://doi.org/10.1016/j.wear.2010.03.029
53. Nosonovsky M, Bhushan B (2012) Lotus Versus Rose: Biomimetic Surface Effects. Green Tribology: Biomimetics, Energy Conservation and Sustainability. Green Tribology Springer, Berlin, pp 25–40.
54. Wang S, Zhang Y, Abidi N, Cabrales L (2009) Wettability and surface free energy of graphene films. Langmuir 25:11078. https://doi.org/10.1021/la901402f
55. Feng C, Yi Z, She F et al (2016) Superhydrophobic and superoleophilic micro-wrinkled reduced graphene oxide as a highly portable and recyclable oil sorbent. ACS Appl Mater Interfaces 8:9977. https://doi.org/10.1021/acsami.6b01648
56. Meier GH (2014) Thermodynamics of Surfaces and Interfaces: Concepts in Inorganic Materials. Cambridge University Press and the Materials Research Society 251 pages, ISBN 9780521879088. MRS Bulletin;40:371–2. Epub 04/01.
57. Yaneva Z, Koumanova B (2006) Comparative modelling of mono- and dinitrophenols sorption on yellow bentonite from aqueous solutions. J Colloid Interface Sci 293:303. https://doi.org/10.1016/j.jcis.2005.06.069
58. Gui X, Li H, Wang K et al (2011) Recyclable carbon nanotube sponges for oil absorption. Acta Mater 59:4798. https://doi.org/10.1016/j.actamat.2011.04.022
59. Hu H, Zhao Z, Gogotsi Y, Qiu J (2014) Compressible carbon nanotube–graphene hybrid aerogels with superhydrophobicity and superoleophilicity for oil sorption. Environ Sci Technol Lett 1:214. https://doi.org/10.1021/ez500021w
60. Park JH, Aluru N (2009) Temperature-dependent wettability on a titanium dioxide surface. Molecular. Simulation 35:31. https://doi.org/10.1080/08927020802398884
61. Li S, Huang J, Ge M et al (2015) Robust Flower-Like TiO_2@Cotton Fabrics with Special Wettability for Effective Self-Cleaning and Versatile Oil/Water Separation. Adv Mater Interfaces 2:1500220. https://doi.org/10.1002/admi.201500220
62. Hu X, Yu Y, Zhou J et al (2015) The improved oil/water separation performance of graphene oxide modified Al_2O_3 microfiltration membrane. J Membr Sci 476:200. https://doi.org/10.1016/j.memsci.2014.11.043
63. Cortese B, Caschera D, Federici F, Ingo GM, Gigli G (2014) Superhydrophobic fabrics for oil-water separation through a diamond-like carbon (DLC) coating. J Mater Chem A 2:6781. https://doi.org/10.1039/C4TA00450G
64. Zang D, Liu F, Zhang M, Niu X, Gao Z, Wang C (2015) Superhydrophobic coating on fiberglass cloth for selective removal of oil from water. Chem Eng J 262:210. https://doi.org/10.1016/j.cej.2014.09.082
65. Zhu T, Li S, Huang J, Mihailiasa M, Lai Y (2017) Rational design of multi-layered superhydrophobic coating on cotton fabrics for UV shielding, self-cleaning and oil-water separation. Mater Des 134:342. https://doi.org/10.1016/j.matdes.2017.08.071